Article

Journal of Vibration and Control
2015, Vol. 21(8) 1639–1656

DOI: 10.1177/1077546313494216
jvc.sagepub.com

Comparison of the four rod theories of longitudinally vibrating rods

C Mei

Abstract

Dynamics of a longitudinally vibrating rod are analyzed from a wave standpoint, in which the motion of the rod is described in terms of waves that propagate through the uniform rod and are reflected and transmitted at structural discontinuities and boundaries. This study is based on the four engineering theories, namely, the elementary, Love, Mindlin–Herrmann, and three-mode theories. The propagation relations that are governed by the equations of motion are derived. The reflection and transmission relations, which are dependent upon the continuity and equilibrium conditions at structural discontinuities, are obtained. Waves generated by externally applied forces are found. The wave propagation, reflection, and transmission relations are assembled to provide a concise and systematic approach to vibration analysis of rods. Numerical examples are presented. Comparisons and recommendations are made for meaningful engineering practice.

Keywords

Longitudinal wave vibration, elementary theory, Love theory, Mindlin–Herrmann theory, three-mode theory

1. Introduction

There exist four main engineering theories for longitudinally vibrating rods: the elementary, Love, Mindlin–Herrmann, and three-mode theories. The governing differential equations vary from one partial differential equation to three coupled partial differential equations. The difficulty level of applying the conventional modal approach (Meirovitch, 2001) to analyzing longitudinal vibrations in a distributed structure increases considerably with the increased complexity of the adopted vibration theory. As a result, most related studies have been confined to the use of elementary or Love theory, the uses of which may result in erroneous analytical results and inappropriate engineering practice.

In this paper, an alternative approach to the conventional modal approach, namely, the wave vibration approach, is adopted for analyzing longitudinal vibrations in rods based on the four engineering theories. Wave approaches are particularly useful in describing the behavior of one-dimensional components in a structure, where a finite number of waves with given directions of propagation exists.

From a wave standpoint, the motion of a rod is described in terms of waves that propagate through the uniform rod and are reflected and transmitted at structural discontinuities and boundaries (Graff, 1975; Mace, 1984; Doyle, 1989; Cremer et al., 2005). The propagation relations are governed by the equations of motion, and the reflection and transmission relations are dependent upon the continuity and equilibrium conditions at the discontinuities. Assembling these wave propagation, reflection, and transmission relations provides a concise and systematic approach to vibration analysis. The author has successfully applied the wave vibration approach in analyzing vibrations of simple and built-up beam and frame structures (Mei, 2005, 2010, 2012, 2013.

Krawczuk et al. (2006) applied the spectral element method (Doyle, 1989) in studying the time domain wave propagation phenomena in uniform rods using the four theories. It was found that the differences in the time domain wave propagation behavior are similar

Department of Mechanical Engineering, The University of Michigan - Dearborn, Dearborn, MI, USA

Received: 7 February 2013; accepted: 13 May 2013

Corresponding author:
C Mei, Department of Mechanical Engineering, The University of Michigan - Dearborn, 4901 Evergreen Road, Dearborn, MI 48128, USA.
Email: cmei@umich.edu

at lower excitation frequencies; however, at high-frequency excitation, these differences are considerable. In this paper, longitudinal vibrations of rods are analyzed using the wave vibration approach based on the four engineering theories. The frequency domain characteristics are examined over a broad frequency band to compare the responses at various frequency ranges. The complexity, from the wave vibration standpoint, is reflected in the number of vibration wave components involved. In the elementary model, only one pair of vibration waves exists in the rod; while in the three-mode elastic model, there exist three pairs of vibration waves. Since the same assembling procedure applies regardless of the number of wave components, the difficulty level involved in wave analysis is much lower than that in conventional modal analysis.

This paper is organized as follows. In the next section, the equations of motion and wave propagation relations are presented. In Section 3, the reflection and transmission matrices at a structural discontinuity caused by a cross-sectional change, as well as the reflections at classical clamped and free boundaries are derived. In Section 4, waves generated by externally applied forces are derived. In Section 5, the propagation, reflection, and transmission matrices are assembled to provide a concise and systematic approach for analyzing longitudinal vibrations in rods. This approach is illustrated using two numerical examples, namely, vibration analysis of a uniform and a stepped rod. Concluding remarks are given in Section 6.

2. Equations of motion and wave propagation

The elementary theory assumes that the axial deformations along the neutral axis of the rod are the same at all points of the cross-section and that there are no transverse deflections. The Love theory assumes that each material point of the rod has a transverse velocity. As a result, while the strain energy is the same as for the Elementary rod theory, the kinetic energy has additional terms (Love, 1927). The Mindlin–Herrmann theory takes into account the lateral displacements by considering the Poisson effect between axial and transverse deformations. It assumes uniform distribution of the axial displacement in the cross-section of the rod (Mindlin and Herrmann, 1951). The three-mode rod theory assumes a parabolic distribution of the longitudinal displacement along the cross-section. It models the longitudinal displacement, the transverse contraction, and the parabolic distribution of the axial displacement along the cross-section (Viktorow, 1967).

The equations of motion and wave propagation relations are presented below; definitions of symbols can be found in the nomenclature.

2.1. Elementary theory

The equation of motion for free longitudinal vibrations according to the elementary theory can be found in standard vibration textbooks (such as Inman, 1994):

$$EA\frac{\partial^2 u(x,t)}{\partial x^2} - \rho A\frac{\partial^2 u(x,t)}{\partial t^2} = 0 \tag{1}$$

Assuming time harmonic motion and using separation of variables, the solution to Equation (1) can be written in the form $u(x,t) = u_0 e^{-ikx} e^{i\omega t}$. Substituting it into Equation (1) gives the longitudinal wavenumber, which is a function of frequency ω,

$$k = \sqrt{\frac{\rho}{E}}\omega \tag{2}$$

With the time dependence $e^{i\omega t}$ suppressed, the solution to Equation (1) can be written as

$$u(x) = c^+ e^{-ikx} + c^- e^{ikx} \tag{3}$$

Consider two points A and B on a uniform rod located a distance x apart, as shown in Figure 1. Waves propagate from one point to the other, with the propagation being determined by the appropriate wavenumber. Denoting the positive and negative going wave vectors at points A and B as a^+ and a^- and b^+ and b^-, respectively, they are related by

$$a^- = f(x)b^- \quad \text{and } b^+ = f(x)a^+ \tag{4}$$

where $f(x) = e^{-ikx}$ is the propagation coefficient for distance x.

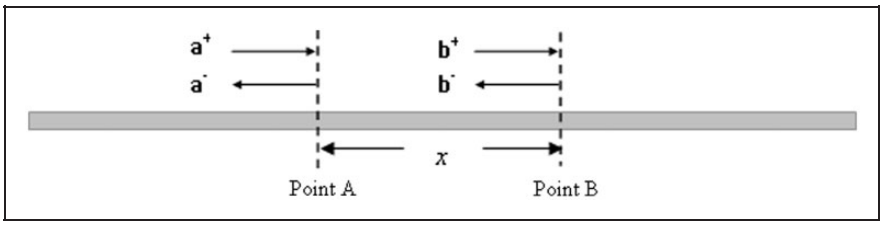

Figure 1. Wave propagation between two points A and B.

2.2. Love theory

The equation of motion for free longitudinal vibrations according to Love theory is (Love, 1927)

$$EA\frac{\partial^2 u_0}{\partial x^2}+\nu^2\rho J\frac{\partial^2}{\partial x^2}\left(\frac{\partial^2 u_0}{\partial t^2}\right)-\rho A\frac{\partial^2 u_0}{\partial t^2}=0 \qquad (5)$$

Following a similar procedure to that described in Section 2.1, the wavenumber is

$$k=\omega\sqrt{\frac{\rho A}{EA-\nu^2\rho J\omega^2}} \qquad (6)$$

With the time dependence $e^{i\omega t}$ suppressed, the solution to Equation (5) is found to be of the same form as described by Equation (3), and the wave propagation relation is the same as that of Equation (4). The only difference is in the wavenumber, which is now given by Equation (6).

2.3. Mindlin–Herrmann theory

The equations of motion for free longitudinal vibrations according to Mindlin–Herrmann theory are (Mindlin and Herrmann, 1951)

$$\begin{aligned}&(2\mu+\lambda)A\frac{\partial^2 u(x,t)}{\partial x^2}+\lambda A\frac{\partial \psi(x,t)}{\partial x}=\rho A\frac{\partial^2 u(x,t)}{\partial t^2},\\&\mu IK_1\frac{\partial^2 \psi(x,t)}{\partial x^2}-(2\mu+\lambda)A\psi(x,t)-\lambda A\frac{\partial u(x,t)}{\partial x}\\&=\rho IK_2\frac{\partial^2 \psi(x,t)}{\partial t^2}\end{aligned} \qquad (7)$$

Again assuming time harmonic motion and using separation of variables, the solutions to Equation (7) can be written in the form $u(x,t)=u_0e^{-ikx}e^{i\omega t}$, and $\psi(x,t)=\psi_0e^{-ikx}e^{i\omega t}$. Substituting these expressions into Equation (7) gives

$$\begin{bmatrix}-k^2(2\mu+\lambda)A+\rho A\omega^2 & -ik\lambda A\\ ik\lambda A & -k^2\mu IK_1-(2\mu+\lambda)A+\rho IK_2\omega^2\end{bmatrix}\times\begin{bmatrix}u_0\\ \psi_0\end{bmatrix}=\begin{bmatrix}0\\0\end{bmatrix} \qquad (8)$$

Setting the determinant of the coefficient matrix of Equation (8) to zero, one obtains the characteristic equation

$$a_2k^4+a_1k^2+a_0=0 \qquad (9)$$

where

$$\begin{aligned}a_2&=(2\mu+\lambda)A\mu IK_1,\\a_1&=4\mu(\mu+\lambda)A^2-\rho IK_2\omega^2(2\mu+\lambda)\\&\quad\times A-\rho A\omega^2\mu IK_1,\\a_0&=-\rho A\omega^2\left[(2\mu+\lambda)A-\rho IK_2\omega^2\right].\end{aligned}$$

It is a quadratic equation in terms of k^2; as a result (unlike the elementary and Love theories), Mindlin–Herrmann theory predicts two modes, with wavenumbers k_1 and k_2, respectively.

There exists a cut-off frequency, which can be solved for by setting k in the characteristic equation (9) to zero. It is

$$\omega_c=\sqrt{\frac{(2\mu+\lambda)A}{\rho IK_2}} \qquad (10)$$

With the time dependence $e^{i\omega t}$ suppressed, the solution to Equation (7) can be written as

$$\begin{aligned}u_0&=a_1^+e^{-ik_1x}+a_2^+e^{-ik_2x}+a_1^-e^{ik_1x}+a_2^-e^{ik_2x},\\\psi_0&=\overline{a_1^+}e^{-ik_1x}+\overline{a_2^+}e^{-ik_2x}+\overline{a_1^-}e^{ik_1x}+\overline{a_2^-}e^{ik_2x}\end{aligned} \qquad (11)$$

The wave amplitudes a of $u(x,t)$ and $\overline{a}$ of $\psi(x,t)$ are related to each other, and the relation can be found from Equation (8) as

$$\frac{\overline{a_1^+}}{a_1^+}=-iP_1;\ \frac{\overline{a_1^-}}{a_1^-}=+iP_1;\ \frac{\overline{a_2^+}}{a_2^+}=-iP_2;\ \frac{\overline{a_2^-}}{a_2^-}=+iP_2 \qquad (12)$$

where

$$P_1=\frac{-k_1^2(2\mu+\lambda)+\rho\omega^2}{k_1\lambda}\ \text{and}\ P_2=\frac{-k_2^2(2\mu+\lambda)+\rho\omega^2}{k_2\lambda}.$$

Hence Equation (11) can be rewritten as

$$\begin{aligned}u_0&=a_1^+e^{-ik_1x}+a_2^+e^{-ik_2x}+a_1^-e^{ik_1x}+a_2^-e^{ik_2x},\\\psi_0&=-iP_1a_1^+e^{-ik_1x}-iP_2a_2^+e^{-ik_2x}+iP_1a_1^-e^{ik_1x}+iP_2a_2^-e^{ik_2x}\end{aligned} \qquad (13)$$

The propagation relations are similar to Equation (4). However, since there exist two wave components, $\mathbf{a}^\pm$ and $\mathbf{b}^\pm$ are now two-by-one vectors, and $\mathbf{f}(x)$ becomes a two-by-two propagation matrix as follows

$$\mathbf{a}^\pm=\begin{bmatrix}a_1^\pm\\a_2^\pm\end{bmatrix},\mathbf{b}^\pm=\begin{bmatrix}b_1^\pm\\b_2^\pm\end{bmatrix}\ \text{and}\ \mathbf{f}(x)=\begin{bmatrix}e^{-ik_1x}&0\\0&e^{-ik_2x}\end{bmatrix} \qquad (14)$$

2.4. Three-mode theory

The equations of motion for free longitudinal vibrations according to the three-mode theory are (Viktorow, 1967):

$$
\begin{aligned}
&(2\mu+\lambda)A\frac{\partial^2 u(x,t)}{\partial x^2}+\lambda A\frac{\partial \psi(x,t)}{\partial x}=\rho A\frac{\partial^2 u(x,t)}{\partial t^2},\\
&\mu I\frac{\partial^2 \psi(x,t)}{\partial x^2}-(2\mu+\lambda)A\psi(x,t)-\lambda A\frac{\partial u(x,t)}{\partial x}\\
&\quad-2\mu Ah\frac{\partial \phi(x,t)}{\partial x}=\rho I\frac{\partial^2 \psi(x,t)}{\partial t^2},\\
&(2\mu+\lambda)I\frac{\partial^2 \phi(x,t)}{\partial x^2}-5\mu A\phi(x,t)+\frac{10}{48}\mu Ah\frac{\partial \psi(x,t)}{\partial x}\\
&=\rho I\frac{\partial^2 \phi(x,t)}{\partial t^2}.
\end{aligned}
\tag{15}
$$

Assuming time harmonic motion and using separation of variables, the solutions to Equation (15) can be written in the form $u(x,t)=u_0e^{-ikx}e^{i\omega t}$, $\psi(x,t)=\psi_0e^{-ikx}e^{i\omega t}$, and $\phi(x,t)=\phi_0e^{-ikx}e^{i\omega t}$. Substituting these expressions into Equation (15) gives

$$
\begin{bmatrix}
-(2\mu+\lambda)Ak^2+\rho A\omega^2 & -ik\lambda A & 0\\
ik\lambda A & -\mu Ik^2-(2\mu+\lambda)A+\rho I\omega^2 & 2\mu Ahik\\
0 & -\frac{10}{48}\mu Ahik & -(2\mu+\lambda)Ik^2-5\mu A+\rho I\omega^2
\end{bmatrix}
\begin{bmatrix}u_0\\ \psi_0\\ \phi_0\end{bmatrix}
=\begin{bmatrix}0\\0\\0\end{bmatrix}.
\tag{16}
$$

Setting the determinant of the coefficient matrix of Equation (16) to zero, one obtains the characteristic equation

$$a_3k^6+a_2k^4+a_1k^2+a_0=0, \tag{17}$$

where

$$
\begin{aligned}
a_3&=-AI^2\mu(2\mu+\lambda)^2,\\
a_2&=A(\lambda+2\mu)\left[\begin{matrix}\frac{5}{12}A^2h^2\mu^2-AI\mu(9\mu+4\lambda)\\ +\rho I^2\omega^2(4\mu+\lambda)\end{matrix}\right],\\
a_1&=-20A^3\mu^2(\mu+\lambda)-A^2\rho\omega^2\\
&\quad\times\left[\mu^2\left(\frac{5}{12}Ah^2-23I\right)-I\lambda(\lambda+13\mu)\right]\\
&\quad-AI^2\rho^2\omega^4(2\lambda+5\mu),\\
a_0&=\rho A\omega^2(5A\mu-\rho I\omega^2)[A(2\mu+\lambda)-\rho I\omega^2]
\end{aligned}
$$

It is a cubic equation in terms of k^2. As a result, the three-mode theory predicts three modes, with wavenumbers k_1, k_2, and k_3, respectively.

By setting k in the characteristic equation (17) to zero, one obtains two cut-off frequencies

$$\omega_{c1}=\sqrt{\frac{(2\mu+\lambda)A}{\rho I}}\quad\text{and}\quad\omega_{c2}=\sqrt{\frac{5\mu A}{\rho I}}. \tag{18}$$

With the time dependence $e^{i\omega t}$ suppressed, the solutions to Equation (15) can be written as

$$
\begin{aligned}
u_0&=a_1^+e^{-ik_1x}+a_2^+e^{-ik_2x}+a_3^+e^{-ik_3x}+a_1^-e^{ik_1x}+a_2^-e^{ik_2x}\\
&\quad+a_3^-e^{ik_3x},\\
\Psi_0&=\overline{a_1^+}e^{-ik_1x}+\overline{a_2^+}e^{-ik_2x}+\overline{a_3^+}e^{-ik_3x}+\overline{a_1^-}e^{ik_1x}+\overline{a_2^-}e^{ik_2x}\\
&\quad+\overline{a_3^-}e^{ik_3x},\\
\phi_0&=\overline{\overline{a_1^+}}e^{-ik_1x}+\overline{\overline{a_2^+}}e^{-ik_2x}+\overline{\overline{a_3^+}}e^{-ik_3x}+\overline{\overline{a_1^-}}e^{ik_1x}\\
&\quad+\overline{\overline{a_2^-}}e^{ik_2x}+\overline{\overline{a_3^-}}e^{ik_3x}.
\end{aligned}
\tag{19}
$$

The wave amplitudes a of $u(x,t)$, $\overline{a}$ of $\psi(x,t)$, and $\overline{\overline{a}}$ of $\phi(x,t)$ are related to each other, and the relation can be found from Equation (16) as

$$
\begin{aligned}
&\frac{\overline{a_1^+}}{a_1^+}=-iP_1,\ \frac{\overline{a_2^+}}{a_2^+}=-iP_2,\ \frac{\overline{a_3^+}}{a_3^+}=-iP_3,\ \frac{\overline{a_1^-}}{a_1^-}=iP_1,\\
&\frac{\overline{a_2^-}}{a_2^-}=iP_2,\frac{\overline{a_3^-}}{a_3^-}=iP_3,\\
&\frac{\overline{\overline{a_1^+}}}{a_1^+}=\frac{\overline{\overline{a_1^-}}}{a_1^-}=N_1,\ \frac{\overline{\overline{a_2^+}}}{a_2^+}=\frac{\overline{\overline{a_2^-}}}{a_2^-}=N_2,\ \frac{\overline{\overline{a_3^+}}}{a_3^+}=\frac{\overline{\overline{a_3^-}}}{a_3^-}=N_3,
\end{aligned}
\tag{20}
$$

where

$$
\begin{aligned}
P_i&=\frac{\rho A\omega^2-(2\mu+\lambda)Ak_i^2}{k_i\lambda A},\\
N_i&=\frac{5}{24}\cdot\frac{\mu h}{\lambda}\cdot\frac{\rho A\omega^2-(2\mu+\lambda)Ak_i^2}{\rho I\omega^2-(2\mu+\lambda)Ik_i^2-5\mu A},\\
&\quad\text{and } i=1,2,3
\end{aligned}
$$

Equation (19) can consequently be rewritten as

$$\begin{aligned} u_0 &= a_1^+ e^{-ik_1 x} + a_2^+ e^{-ik_2 x} + a_3^+ e^{-ik_3 x} + a_1^- e^{ik_1 x} + a_2^- e^{ik_2 x} \\ &\quad + a_3^- e^{ik_3 x}, \\ \Psi_0 &= -iP_1 a_1^+ e^{-ik_1 x} - iP_2 a_2^+ e^{-ik_2 x} - iP_3 a_3^+ e^{-ik_3 x} \\ &\quad + iP_1 a_1^- e^{ik_1 x} + iP_2 a_2^- e^{ik_2 x} + iP_3 a_3^- e^{ik_3 x}, \\ \phi_0 &= N_1 a_1^+ e^{-ik_1 x} + N_2 a_2^+ e^{-ik_2 x} + N_3 a_3^+ e^{-ik_3 x} \\ &\quad + N_1 a_1^- e^{ik_1 x} + N_2 a_2^- e^{ik_2 x} + N_3 a_3^- e^{ik_3 x}. \end{aligned} \tag{21}$$

The propagation relations are again similar to Equation (4). Since there exist three wave components, $\mathbf{a}^{\pm}$ and $\mathbf{b}^{\pm}$ are now three-by-one vectors, and $\mathbf{f}(x)$ becomes a three-by-three propagation matrix as follows:

$$\mathbf{a}^{\pm} = \begin{bmatrix} a_1^{\pm} \\ a_2^{\pm} \\ a_3^{\pm} \end{bmatrix}, \mathbf{b}^{\pm} = \begin{bmatrix} b_1^{\pm} \\ b_2^{\pm} \\ b_3^{\pm} \end{bmatrix} \text{ and } \mathbf{f}(x) = \begin{bmatrix} e^{-ik_1 x} & 0 & 0 \\ 0 & e^{-ik_2 x} & 0 \\ 0 & 0 & e^{-ik_3 x} \end{bmatrix} \tag{22}$$

3. Wave reflection and transmission

Waves incident upon discontinuities are reflected and transmitted. Two types of discontinuities are studied. One is caused by a change of cross-section, and the other is due to the termination of a structure, that is, a boundary.

Let two rods of different properties be joined at $x = 0$ as shown in Figure 2. It is assumed that their neutral axes coincide. Owing to impedance mismatching, an incident wave a^+ from one side gives rise to reflected and transmitted waves a^- and b^+ at the junction, which are related to the incident wave through the transmission and reflection coefficients t and r by

$$b^+ = ta^+ \text{ and } a^- = ra^+ \tag{23}$$

The transmission and reflection relation can be found from the continuity and equilibrium conditions at the discontinuity.

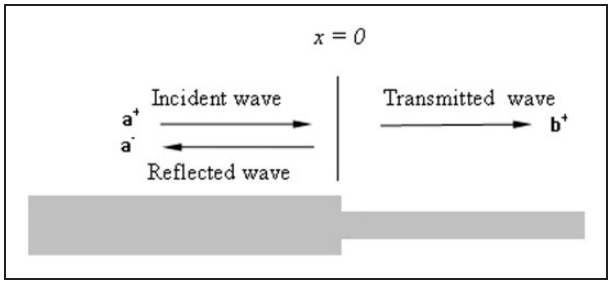

Figure 2. Wave reflection and transmission at a change of cross-section.

A structural discontinuity caused by a general elastic boundary is illustrated in Figure 3. An incident wave is reflected at the boundary. The incident wave $a^+$and the reflected wave a^- are related through the reflection coefficient r by

$$a^- = ra^+ \tag{24}$$

where r can be determined by considering equilibrium at the boundary. Reflection coefficients at a clamped and a free boundary are found, which correspond to the two extreme values of the spring stiffness, that is, infinity and zero, respectively.

3.1. Elementary theory

3.1.1. Reflection and transmission at a change of cross-section. The continuity and equilibrium conditions at the discontinuity are

$$u_L = u_R \quad \text{and } F_L = F_R \tag{25}$$

According to the elementary theory, the axial force and the axial deflection are related by

$$F = EA\frac{\partial u}{\partial x} \tag{26}$$

Assuming that an incident wave arrives from the left side of the cross-section, as shown in Figure 2, Equations (25) and (26) give

$$\begin{aligned} a^+ + a^- &= b^+ \quad \text{and } (EA)_L ik_L a^+ - (EA)_L ik_L a^- \\ &= (EA)_R ik_R b^+ \end{aligned} \tag{27}$$

The transmission and reflection coefficients t and r corresponding to the incident wave from the left can then be solved from Equations (23) and (27).

3.1.2. Reflection at a free and a clamped boundary. At a free boundary, the equilibrium condition is

$$F(x, t) = 0 \tag{28}$$

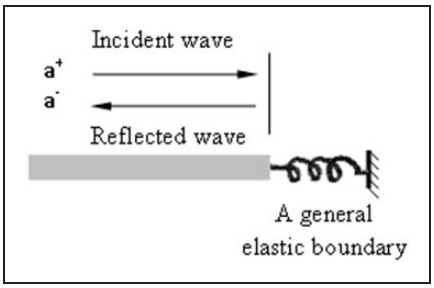

Figure 3. Wave reflection at a boundary.

From Equations (24), (26), and (28), the reflection coefficient is found as

$$r = 1 \tag{29}$$

The equilibrium condition at a clamped boundary is

$$u(x, t) = 0 \tag{30}$$

The reflection coefficient is found from Equations (24) and (30) as

$$r = -1 \tag{31}$$

3.2. Love theory

3.2.1. Reflection and transmission at a change of cross-section. The continuity and equilibrium conditions at the discontinuity are given by the same equations of (25); however, the axial force and the axial deflection are related by

$$F = EA\frac{\partial u}{\partial x} + v^2\rho J\frac{\partial \ddot{u}}{\partial x} \tag{32}$$

The continuity and equilibrium equations corresponding to an incident wave arriving from the left side of the cross-section are

$$\begin{aligned} &a^+ + a^- = b^+, \\ &-k_L\left[(EA)_L - \left(v^2\rho J\right)_L\omega^2\right]a^+ + k_L\left[(EA)_L - \left(v^2\rho J\right)_L\omega^2\right]a^- \\ &= k_R\left[(EA)_R - \omega^2\left(v^2\rho J\right)_R\right]b^+ \end{aligned} \tag{33}$$

The transmission and reflection coefficients t and r corresponding to the incident wave from the left can then be found from Equations (23) and (33).

3.2.2. Reflection at a free and a clamped boundary. The reflection coefficient at a free boundary can be found from Equations (24), (28), and (32). It is given by the same expression as Equation (29), that is, $r = 1$. The reflection coefficient at a clamped boundary is $r = -1$, the same as that of Equation (31).

3.3. Mindlin–Herrmann theory

3.3.1. Reflection and transmission at a change of cross-section. The continuity conditions according to the Mindlin–Herrmann theory at the discontinuity are

$$\mathrm{u}_L = \mathrm{u}_R \quad \text{and } \psi_L = \psi_R \tag{34}$$

and the equilibrium conditions are

$$F_u^L = F_u^R \quad \text{and } F_\psi^L = F_\psi^R \tag{35}$$

The forces and deflections are related as follows:

$$F_u = (2\mu + \lambda)A\frac{\partial u}{\partial x} + \lambda A\psi \quad \text{and } F_\psi = \mu I K_1\frac{\partial \psi}{\partial x} \tag{36}$$

The continuity and equilibrium equations corresponding to an incident wave arriving from the left side of the cross-section are found from Equations (34)–(36) in matrix form as

$$\begin{aligned} &\begin{bmatrix} -1 & -1 \\ iP_{L1} & iP_{L2} \end{bmatrix}\mathbf{a}^+ - \begin{bmatrix} 1 & 1 \\ iP_{L1} & iP_{L2} \end{bmatrix}\mathbf{a}^- = \begin{bmatrix} -1 & -1 \\ iP_{R1} & iP_{R2} \end{bmatrix}\mathbf{b}^+, \\ &\begin{bmatrix} (2\mu_L + \lambda_L)A_L ik_{L1} + \lambda_L A_L iP_{L1} & (2\mu_L + \lambda_L)A_L ik_{L2} + \lambda_L A_L iP_{L2} \\ -(\mu I K_1)_L P_{L1}k_{L1} & -(\mu I K_1)_L P_{L2}k_{L2} \end{bmatrix}\mathbf{a}^+ \\ &\quad - \begin{bmatrix} (2\mu_L + \lambda_L)\mathrm{A}_L ik_{L1} + \lambda_L A_L iP_{L1} & (2\mu_L + \lambda_L)A_L ik_{L2} + \lambda_L A_L iP_{L2} \\ -(\mu I K_1)_L P_{L1}k_{L1} & -(\mu I K_1)_L P_{L2}k_{L2} \end{bmatrix}\mathbf{a}^- \\ &= \begin{bmatrix} (2\mu_R + \lambda_R)A_R ik_{R1} + \lambda_R A_R iP_{R1} & (2\mu_R + \lambda_R)A_R ik_{R2} + \lambda_R A_R iP_{R2} \\ -(\mu I K_1)_R P_{R1}k_{R1} & -(\mu I K_1)_R P_{R2}k_{R2} \end{bmatrix}\mathbf{b}^+ \end{aligned} \tag{37}$$

The transmission and reflection matrices **t** and **r** corresponding to an incident wave from the left can be solved from Equations (23) and (37).

3.3.2. Reflection at a free and a clamped boundary. At a free boundary, the equilibrium conditions are

$$F_u = 0 \quad \text{and } F_\psi = 0 \tag{38}$$

From Equations (24), (36), and (38), the reflection coefficients are found as

$$\mathbf{r} = \begin{bmatrix} \left(\frac{2\mu}{\lambda}+1\right)ik_1 + iP_1 & \left(\frac{2\mu}{\lambda}+1\right)ik_2 + iP_2 \\ P_1k_1 & P_2k_2 \end{bmatrix}^{-1} \times \begin{bmatrix} \left(\frac{2\mu}{\lambda}+1\right)ik_1 + iP_1 & \left(\frac{2\mu}{\lambda}+1\right)\mathrm{i}k_2 + iP_2 \\ -P_1k_1 & -P_2k_2 \end{bmatrix} \tag{39}$$

The equilibrium conditions at a clamped boundary are

$$u = 0 \quad \text{and } \psi = 0 \tag{40}$$

and the equilibrium conditions are

$$F_u^L = F_u^R, \quad F_\psi^L = F_\psi^R, \quad F_\phi^L = F_\phi^R \tag{43}$$

The forces and deflections are related as follows:

$$F_u = (2\mu+\lambda)A\frac{\partial u}{\partial x} + \lambda A\psi,\ F_\psi = \mu I\left(\frac{\partial \psi}{\partial x} - 24\frac{\Phi}{h}\right),\ F_\phi = \frac{48}{5}(2\mu+\lambda)I\frac{\partial \Phi}{\partial x} \tag{44}$$

The continuity and equilibrium equations corresponding to an incident wave arriving from the left side of the cross-section are found from Equations (42)–(44). In matrix form, they are

$$\begin{bmatrix} -1 & -1 & -1 \\ iP_{L1} & iP_{L2} & iP_{L3} \\ -N_{L1} & -N_{L2} & -N_{L3} \end{bmatrix}\mathbf{a}^+ - \begin{bmatrix} 1 & 1 & 1 \\ iP_{L1} & iP_{L2} & iP_{L3} \\ N_{L1} & N_{L2} & N_{L3} \end{bmatrix}\mathbf{a}^- = \begin{bmatrix} -1 & -1 & -1 \\ iP_{R1} & iP_{R2} & iP_{R3} \\ -N_{R1} & -N_{R2} & -N_{R3} \end{bmatrix}\mathbf{b}^+$$

$$\begin{bmatrix} (2\mu_L+\lambda_L)A_Lik_{L1} + \lambda_LA_LiP_{L1} & (2\mu_L+\lambda_L)A_Lik_{L2} + \lambda_LA_LiP_{L2} & (2\mu_L+\lambda_L)A_Lik_{L3} + \lambda_LA_LiP_{L3} \\ \mu_LI_LP_{L1}k_{L1} + \frac{24\mu_LI_LN_{L1}}{h_L} & \mu_LI_LP_{L2}k_{L2} + \frac{24\mu_LI_LN_{L2}}{h_L} & \mu_LI_LP_{L3}k_{L3} + \frac{24\mu_LI_LN_{L3}}{h_L} \\ (2\mu_L+\lambda_L)I_Lik_{L1}N_{L1} & (2\mu_L+\lambda_L)I_Lik_{L2}N_{L2} & (2\mu_L+\lambda_L)I_Lik_{L3}N_{L3} \end{bmatrix}\mathbf{a}^+$$

$$-\begin{bmatrix} (2\mu_L+\lambda_L)A_Lik_{L1} + \lambda_LA_LiP_{L1} & (2\mu_L+\lambda_L)A_Lik_{L2} + \lambda_LA_LiP_{L2} & (2\mu_L+\lambda_L)A_Lik_{L3} + \lambda_LA_LiP_{L3} \\ -\mu_LI_LP_{L1}k_{L1} - \frac{24\mu_LI_LN_{L1}}{h_L} & -\mu_LI_LP_{L2}k_{L2} - \frac{24\mu_LI_LN_{L2}}{h_L} & -\mu_LI_LP_{L3}k_{L3} - \frac{24\mu_LI_LN_{L3}}{h_L} \\ (2\mu_L+\lambda_L)I_Lik_{L1}N_{L1} & (2\mu_L+\lambda_L)I_Lik_{L2}N_{L2} & (2\mu_L+\lambda_L)I_Lik_{L3}N_{L3} \end{bmatrix}\mathbf{a}^-$$

$$=\begin{bmatrix} (2\mu_R+\lambda_R)A_Rik_{R1} + \lambda_RA_RiP_{R1} & (2\mu_R+\lambda_R)A_Rik_{R2} + \lambda_RA_RiP_{R2} & (2\mu_R+\lambda_R)A_Rik_{R3} + \lambda_RA_RiP_{R3} \\ \mu_RI_RP_{R1}k_{R1} + \frac{24\mu_RI_RN_{R1}}{h_R} & \mu_RI_RP_{R2}k_{R2} + \frac{24\mu_RI_RN_{R2}}{h_R} & \mu_RI_RP_{R3}k_{R3} + \frac{24\mu_RI_RN_{R3}}{h_R} \\ (2\mu_R+\lambda_R)I_Rik_{R1}N_{R1} & (2\mu_R+\lambda_R)I_Rik_{R2}N_{R2} & (2\mu_R+\lambda_R)I_Rik_{R3}N_{R3} \end{bmatrix}\mathbf{b}^+ \tag{45}$$

The reflection coefficients are found from Equations (24) and (40) as

$$\mathbf{r} = \begin{bmatrix} 1 & 1 \\ iP_1 & iP_2 \end{bmatrix}^{-1}\begin{bmatrix} -1 & -1 \\ iP_1 & iP_2 \end{bmatrix} \tag{41}$$

3.4. Three-mode theory

3.4.1. Reflection and transmission at a change of cross-section. The continuity conditions according to the three-mode theory at the discontinuity are

$$u_L = u_R, \quad \psi_L = \psi_R, \quad \phi_L = \phi_R \tag{42}$$

The transmission and reflection matrices **t** and **r** corresponding to an incident wave from the left can be solved from Equations (23) and (45).

3.4.2. Reflection at a free and a clamped boundary. At a free boundary, the equilibrium conditions are

$$F_u = 0, \quad F_\psi = 0, \quad F_\phi = 0 \tag{46}$$

From Equations (24), (44), and (46), the reflection matrix is

$$\mathbf{r}=\begin{bmatrix} \left(\frac{2\mu}{\lambda}+1\right)ik_1+iP_1 & \left(\frac{2\mu}{\lambda}+1\right)ik_2+iP_2 & \left(\frac{2\mu}{\lambda}+1\right)ik_3+iP_3 \\ P_1k_1+\frac{24}{h}N_1 & P_2k_2+\frac{24}{h}N_2 & P_3k_3+\frac{24}{h}N_3 \\ ik_1N_1 & ik_2N_2 & ik_3N_3 \end{bmatrix}^{-1} \times \begin{bmatrix} \left(\frac{2\mu}{\lambda}+1\right)ik_1+iP_1 & \left(\frac{2\mu}{\lambda}+1\right)ik_2+iP_2 & \left(\frac{2\mu}{\lambda}+1\right)ik_3+iP_3 \\ -\left(P_1k_1+\frac{24}{h}N_1\right) & -\left(P_2k_2+\frac{24}{h}N_2\right) & -\left(P_3k_3+\frac{24}{h}N_3\right) \\ ik_1N_1 & ik_2N_2 & ik_3N_3 \end{bmatrix} \tag{47}$$

The equilibrium conditions at a clamped boundary are

$$u=0, \quad \psi=0, \quad \Phi=0 \tag{48}$$

The reflection coefficients are found from Equations (24) and (48) as

$$\mathbf{r}=\begin{bmatrix} 1 & 1 & 1 \\ iP_1 & iP_2 & iP_3 \\ N_1 & N_2 & N_3 \end{bmatrix}^{-1}\begin{bmatrix} -1 & -1 & -1 \\ iP_1 & iP_2 & iP_3 \\ -N_1 & -N_2 & -N_3 \end{bmatrix} \tag{49}$$

4. Waves generated by an externally applied point force

An applied force has the effect of injecting waves into a structure. Consider the axial waves injected by a point force $\bar{F}$ applied at $x=0$ as shown in Figure 4. At $x=0$, there are discontinuities in the axial force in the rod with resulting discontinuities in the waves $a^{\pm}$ and $b^{\pm}$ at the point where the excitation force is applied. The relations between the applied force and the waves can be found from the continuity and equilibrium conditions at the point where the force is applied. The detailed expressions corresponding to the various axial vibration theories are derived as follows.

4.1. Elementary theory

The continuity and equilibrium conditions are

$$u^-=u^+ \quad \text{and } \overline{F_u}=F_u^- - F_u^+ \tag{50}$$

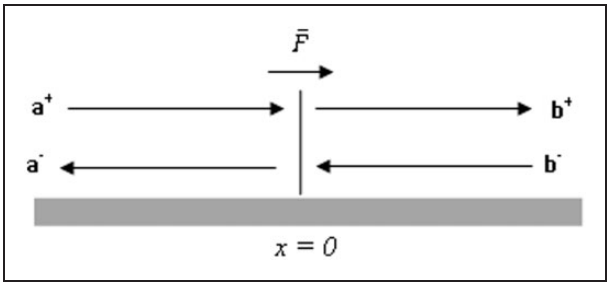

Figure 4. Force-generated waves.

The relations between the applied force and the waves are found from Equations (26) and (50) as

$$b^+-a^+=-i\frac{\bar{F}}{2EAk} \quad \text{and } b^--a^-=i\frac{\bar{F}}{2EAk}. \tag{51}$$

4.2. Love theory

The continuity and equilibrium conditions are the same as Equation (50). The relations between the applied force and the waves are found from Equations (32) and (50) as

$$b^+-a^+=-i\frac{\overline{F_u}}{2(EA-\nu^2\rho J\omega^2)k} \quad \text{and} \quad b^--a^-=i\frac{\overline{F_u}}{2(EA-\nu^2\rho J\omega^2)k} \tag{52}$$

4.3. Mindlin–Herrmann Theory

The continuity conditions are

$$u^+=u^- \quad \text{and } \psi^+=\psi^- \tag{53}$$

The equilibrium conditions are

$$\overline{\mathrm{F}_u}=F_u^- - F_u^+ \quad \text{and } \overline{F_\psi}=F_\psi^- - F_\psi^+ \tag{54}$$

The relations between the applied force and the force-generated waves are found from Equations (36), (53), and (54) as

$$\mathbf{b}^+-\mathbf{a}^+=\begin{bmatrix} i\frac{AF_\psi\lambda(P_1k_2-P_2k_1)+2AF_\psi\mu(P_1k_2-P_2k_1)+K_1F_uP_2\mu(P_2k_2-P_1k_1)}{2K_1A\mu(\lambda+2\mu)(k_1^2P_1P_2+k_2^2P_1P_2-P_1^2k_1k_2-P_2^2k_1k_2)} \\ i\frac{AF_\psi\lambda(P_1k_2-P_2k_1)+2AF_\psi\mu(P_1k_2-P_2k_1)+K_1F_uP_1\mu(P_2k_2-P_1k_1)}{2K_1A\mu(\lambda+2\mu)(k_1^2P_1P_2+k_2^2P_1P_2-P_1^2k_1k_2-P_2^2k_1k_2)} \end{bmatrix},$$
$$\mathbf{b}^--\mathbf{a}^-=\begin{bmatrix} i\frac{AF_\psi\lambda(P_1k_2-P_2k_1)+2AF_\psi\mu(P_1k_2-P_2k_1)-K_1F_uP_2\mu(P_2k_2-P_1k_1)}{2K_1A\mu(\lambda+2\mu)(k_1^2P_1P_2+k_2^2P_1P_2-P_1^2k_1k_2-P_2^2k_1k_2)} \\ i\frac{AF_\psi\lambda(P_1k_2-P_2k_1)+2AF_\psi\mu(P_1k_2-P_2k_1)-K_1F_uP_1\mu(P_2k_2-P_1k_1)}{2K_1A\mu(\lambda+2\mu)(k_1^2P_1P_2+k_2^2P_1P_2-P_1^2k_1k_2-P_2^2k_1k_2)} \end{bmatrix}. \tag{55}$$

4.4. Three-mode theory

The continuity conditions are

$$u^+ = u^-, \quad \psi^+ = \psi^-, \quad \phi^+ = \phi^- \tag{56}$$

The equilibrium conditions are

$$\overline{\mathrm{F}_u} = F_u^- - F_u^+, \ \overline{\mathrm{F}_\psi} = F_\psi^- - F_\psi^+, \ \overline{F_\Phi} = F_\Phi^- - F_\Phi^+ \tag{57}$$

The relations between the applied force and the waves are found from Equations (44), (56), and (57) in a similar form; however, the expressions are too lengthy to be presented.

5. Vibration analysis using the wave approach

Vibration analysis of an axially vibrating rod from a wave standpoint involves a concise and systematic assembling procedure using the propagation, transmission, reflection, and waves injected by externally applied force expressions. This approach is illustrated through two numerical examples below, namely, vibration analysis of a uniform and a stepped rod.

5.1. Vibration analysis of a uniform rod

Figure 5 illustrates a rod with an external excitation point force applied at C. There exist the following propagation and reflection relations:

- At boundaries A and B

$$\mathbf{a}^+ = \mathbf{r}_A \mathbf{a}^- \quad \text{and } \mathbf{b}^- = \mathbf{r}_B \mathbf{b}^+ \tag{58}$$

where $\mathbf{r}_A$ and $\mathbf{r}_B$ are the reflection matrices at the boundaries.

- At point C

$$\mathbf{c}_2^+ - \mathbf{c}_1^+ = \mathbf{q}_1 \quad \text{and } \mathbf{c}_1^- - \mathbf{c}_2^- = \mathbf{q}_2 \tag{59}$$

where $\mathbf{q}_1$ and $\mathbf{q}_2$ represent the right-hand side expressions of Equations (51), (52), (55), etc.

- The propagation relations are

$$\mathbf{c}_1^+ = \mathbf{f}(L_1)\mathbf{a}^+, \quad \mathbf{a}^- = \mathbf{f}(L_1)\mathbf{c}_1^-, \quad \mathbf{b}^+ = \mathbf{f}(L_2)\mathbf{c}_2^+, \quad \mathbf{c}_2^- = \mathbf{f}(L_2)\mathbf{b}^- \tag{60}$$

Assembling these propagation, reflection, and transmission relations and putting them in matrix form, one has

$$\mathbf{A}_f \mathbf{z}_f = \mathbf{F} \tag{61}$$

where $\mathbf{A}_f$ is a square coefficient matrix, $\mathbf{z}_f$ is the wave component vector, and $\mathbf{F}$ is a vector related to the externally applied force.

From Equation (61), one obtains the deflection of any point along the rod. For example, the deflection of a point located between boundary A and the excitation point C that is a distance x from C is given by

$$x = \begin{bmatrix} 1 & 1 \end{bmatrix} \mathbf{f}(x)\mathbf{c}_1^- + \begin{bmatrix} 1 & 1 \end{bmatrix} \mathbf{f}(-x)\mathbf{c}_1^+ \tag{62}$$

Similarly, the deflection of a point located between boundary B and the excitation point C that is a distance x from C is given by

$$x = \begin{bmatrix} 1 & 1 \end{bmatrix} \mathbf{f}(x)\mathbf{c}_2^- + \begin{bmatrix} 1 & 1 \end{bmatrix} \mathbf{f}(-x)\mathbf{c}_2^+ \tag{63}$$

5.2. Vibration analysis of a stepped rod

Figure 6 shows the stepped rod involving a geometric discontinuity at D and a point force applied at C. In addition to the boundary reflection relations of Equation (58) and the force- generated waves relations

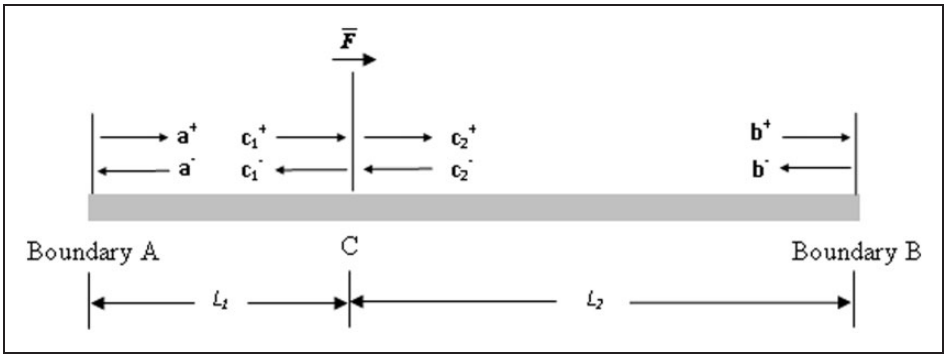

Figure 5. Wave propagation, reflection, and transmission in a uniform rod.

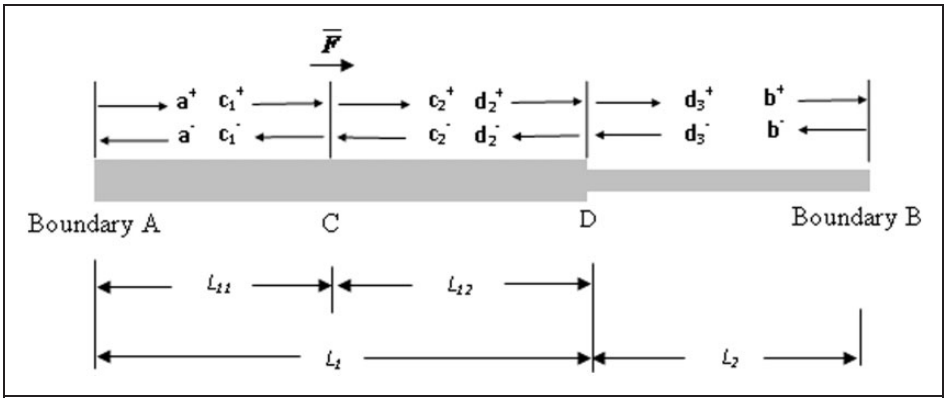

Figure 6. Wave propagation, reflection, and transmission in a stepped rod.

of Equation (59), there exist the following propagation, transmission, and reflection relations:

- At the geometric discontinuity D

$$\mathbf{d}_2^- = \mathbf{r}_{LL}\mathbf{d}_2^+ + \mathbf{t}_{RL}\mathbf{d}_3^- \quad \text{and } \mathbf{d}_3^+ = \mathbf{r}_{RR}\mathbf{d}_3^- + \mathbf{t}_{LR}\mathbf{d}_2^+. \quad (64)$$

- The propagation relations are

$$\begin{aligned} &\mathbf{c}_1^+ = \mathbf{f}(L_{11})\mathbf{a}^+, \quad \mathbf{a}^- = \mathbf{f}(L_{11})\mathbf{c}_1^-, \quad \mathbf{d}_2^+ = \mathbf{f}(L_{12})\mathbf{c}_2^+, \\ &\mathbf{c}_2^- = \mathbf{f}(L_{12})\mathbf{d}_2^-, \quad \mathbf{b}^+ = \mathbf{f}(L_2)\mathbf{d}_3^+, \quad \mathbf{d}_3^- = \mathbf{f}(L_2)\mathbf{b}^-. \end{aligned} \quad (65)$$

Equations (58), (59), (64), and (65) can be assembled into the matrix form of Equation (61), from which the deflections of any point along the rod can be obtained.

5.3. Numerical examples

The physical parameters are chosen to be the same as those of Krawczuk et al. (2006). The material properties of the steel rod are as follows: Young's modulus 210 GPa, Poisson ratio 0.3, and mass density 7850 kg/m^3. Both the uniform and the stepped rod are assumed clamped at one end and free at the other. The dimensions of the uniform rod are as follows: length 4.00 m, width 0.02 m, and thickness 0.02 m. The stepped rod is assumed to be of the same length, with a step change in the thickness of the rod from 0.02 to 0.01 m at midspan.

5.3.1. Spectrum relations. Figures 7–9 illustrate the frequency dependence of the wavenumbers based on the four axial vibration theories. The elementary and Love theories predict a single mode and the Mindlin–Herrmann and three-mode theories predict two and three modes, respectively.

As shown in Figure 7, the single wavenumber predicted by the elementary and Love theories is real. This corresponds to a single pair of propagation waves in an axially vibration rod. The predictions from the two theories agree well with each other up to considerably high frequencies. This, however, does not imply that both theories are accurate to this frequency level, as will be seen in the frequency responses in the coming subsections.

Figure 8 shows the two wave numbers predicted by the Mindlin–Herrmann theory. One of the wavenumbers is always real. The root situation of the other depends on the frequency range: below the cut-off frequency of Equation (10), it is purely imaginary; while above the cut-off frequency, it becomes real. This indicates that below the cut-off frequency, there exist a pair of propagation waves and a pair of decaying waves in an axially vibration rod; and above the cut-off frequency, there exist two pairs of propagation waves in the rod.

The root situation of the three wavenumbers predicted by the three-mode theory is quite complicated, as shown in Figure 9. First, there are two predicted cut-off frequencies as shown in Equation (18). As a result, there exist two sets of wave mode transitions and a pseudo-cut-off frequency. The additional pseudo-cut-off frequency and the two predicted cut-off frequencies are marked using vertical lines in Figure 9. For the given example rod, their values are 163, 165, and 198 kHz, respectively. To have a better view of the wave mode transition and the cut-off frequencies, a zoomed in plot of Figure 9 is presented in Figure 10. It is clear that there is a wave mode transition at this pseudo-cut-off frequency of 163 kHz. The wave mode between this pseudo cut-off frequency and the lower predicted cut-off frequency is similar to that above the higher predicted cut-off frequency. As described earlier, the two real

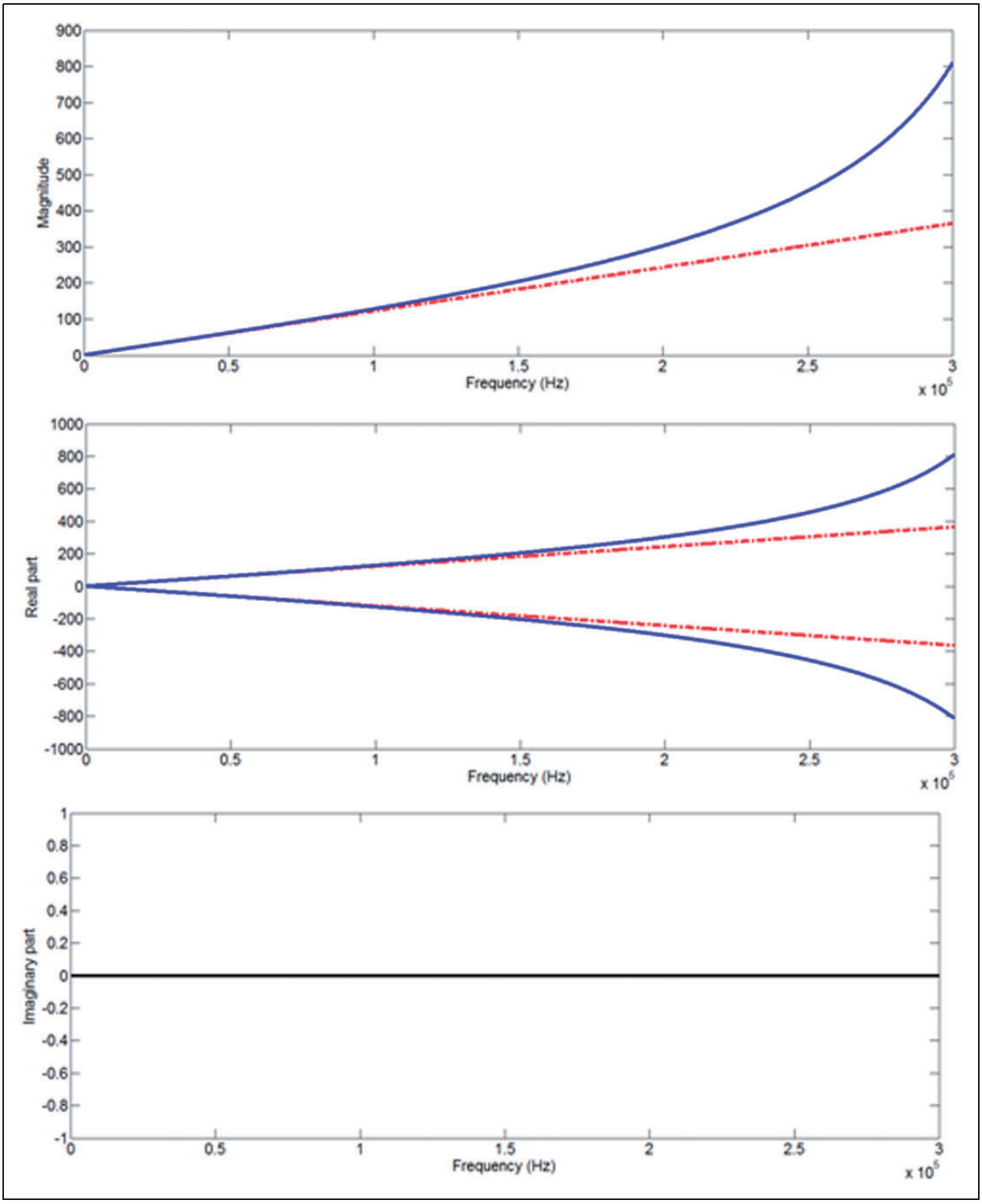

Figure 7. Magnitude, real part, and imaginary part of the single wavenumber by the elementary (-·-·-) and Love (—) theories.

cut-off frequencies are obtained by setting the characteristic equation of Equation (17) to zero. Then where does this pseudo-cut-off frequency come? Interestingly, this pseudo-cut-off frequency is also related to the characteristic equation of Equation (17). Consider the discriminant, Δ, of the left-hand side of Equation (17):

$$\Delta = 18a_3a_2a_1a_0 - 4a_2^3a_0 + a_2^2a_1^2 - 4a_3a_1^3 - 27a_3^2a_0^2, \quad (66)$$

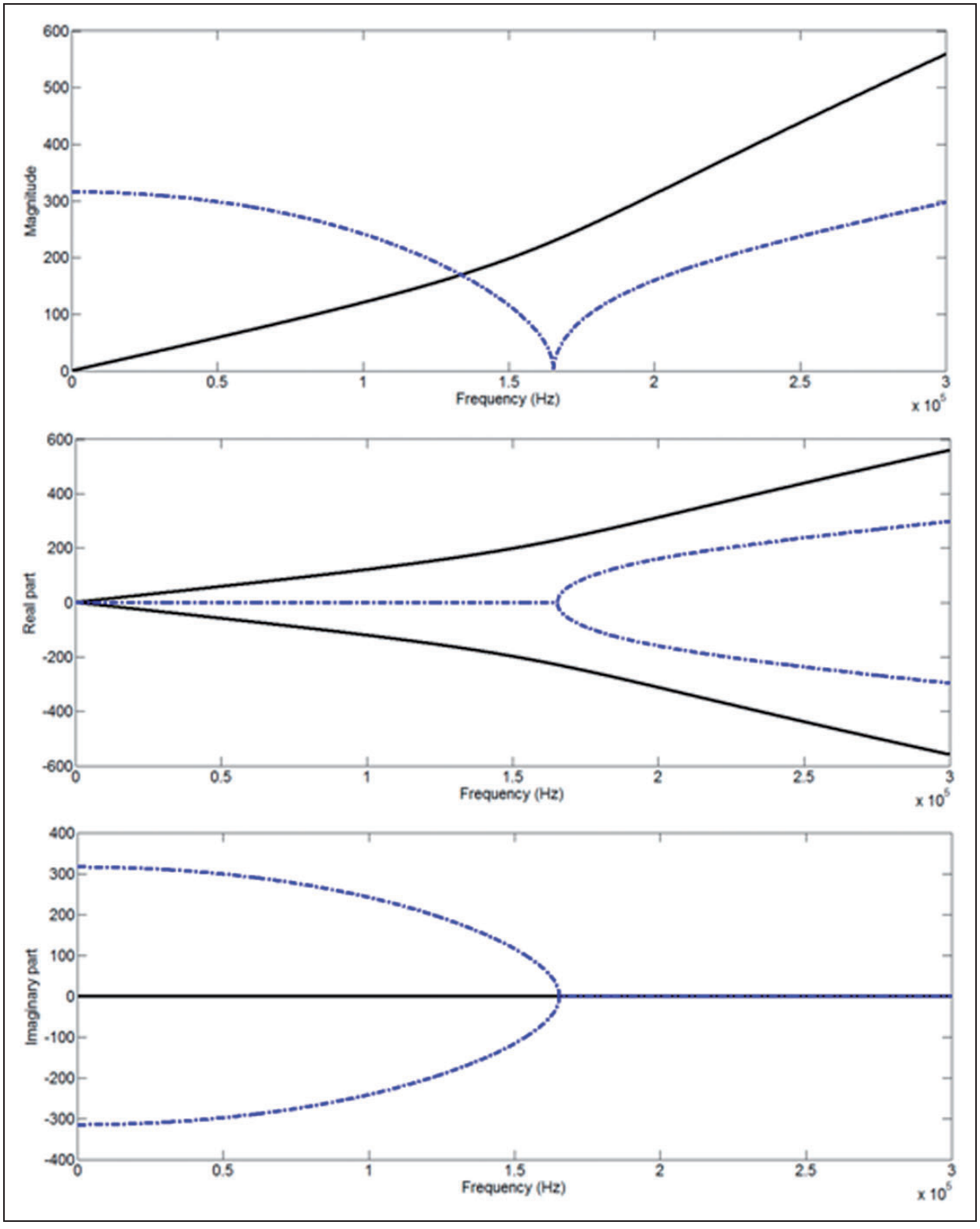

Figure 8. Magnitude, real part, and imaginary part of the two wavenumbers by Mindlin–Herrmann theory.

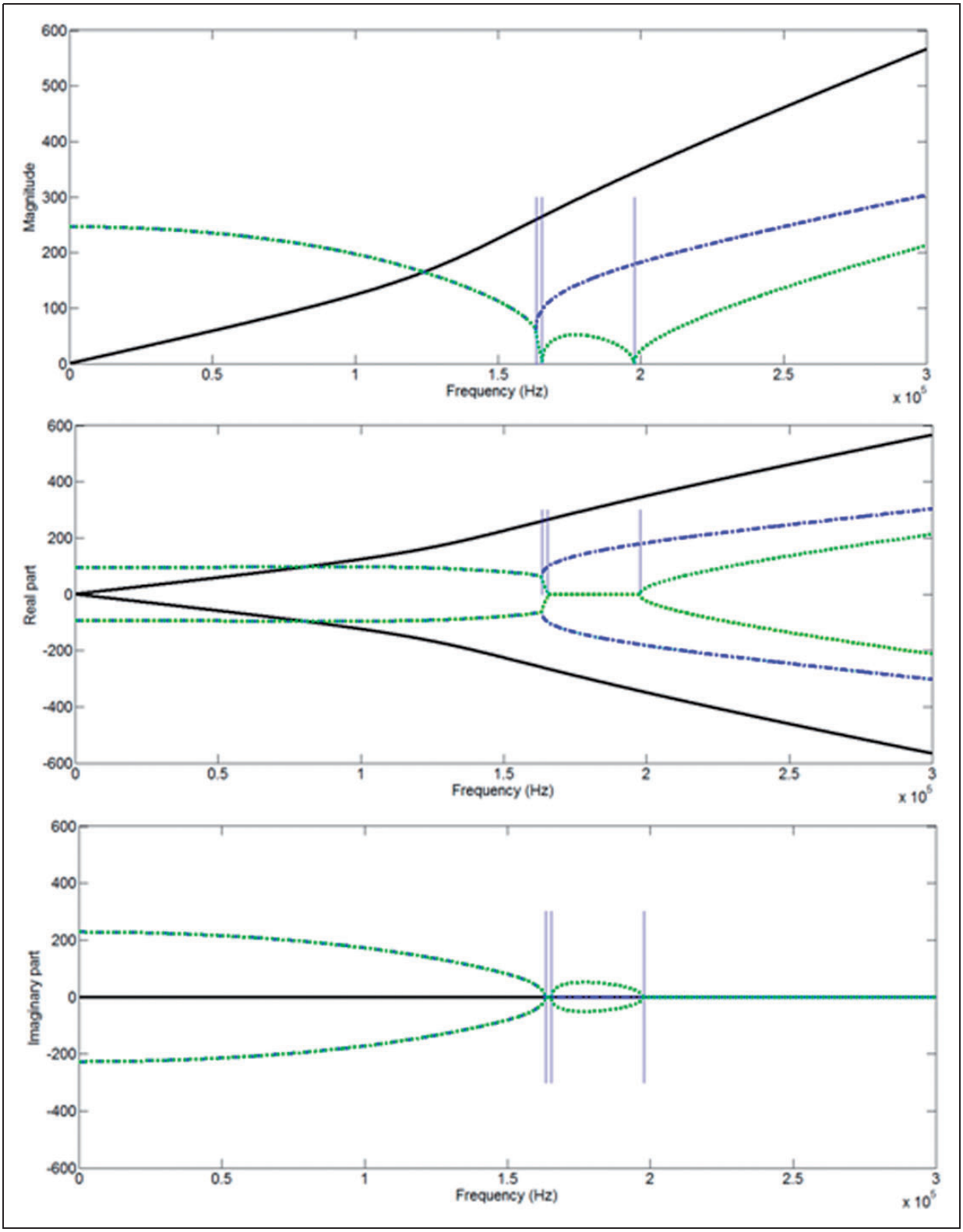

Figure 9. Magnitude, real part, and imaginary part of the three wavenumbers by the three-mode theory.

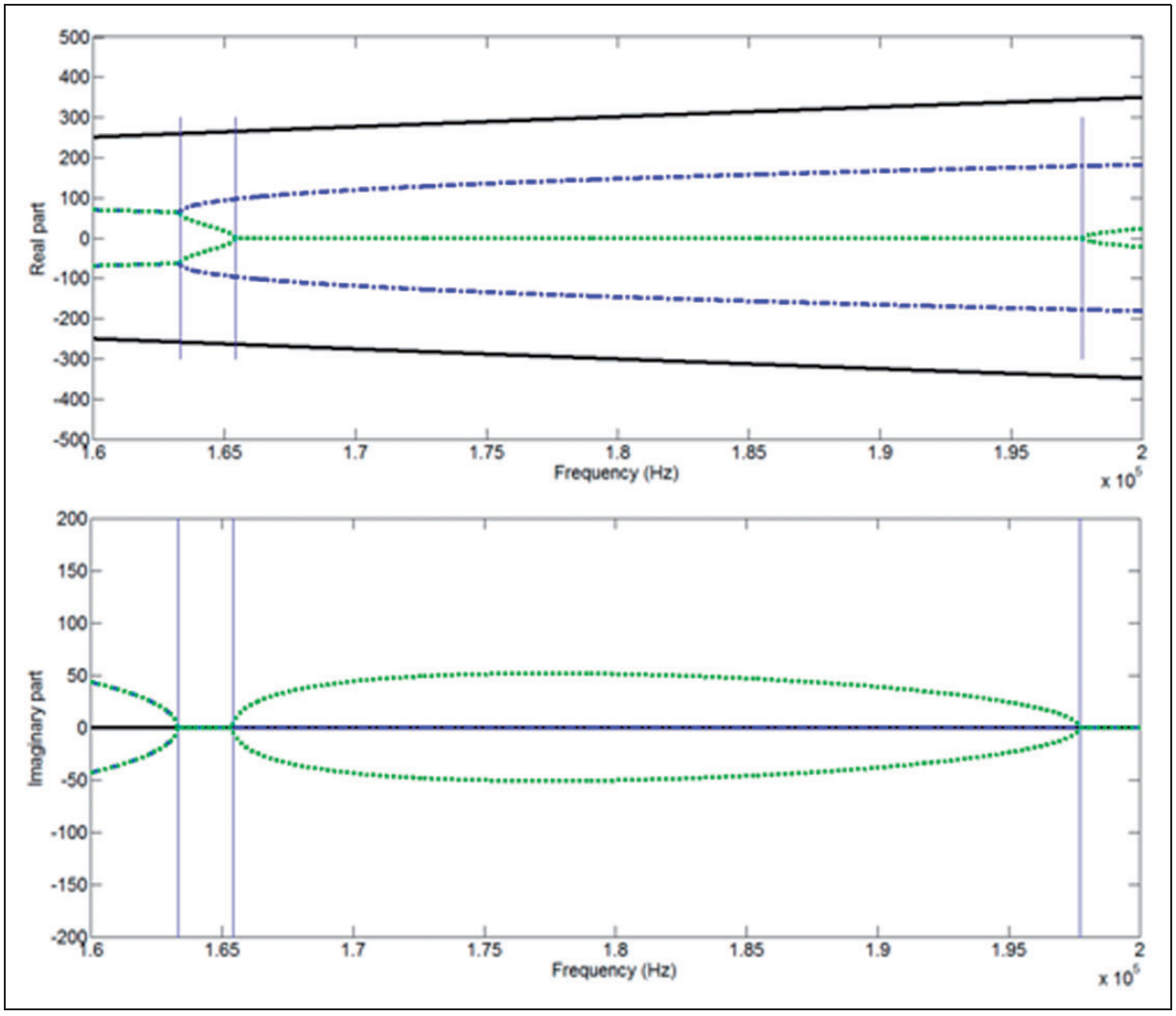

Figure 10. Enlarged view of the real part and imaginary part of the three wavenumbers by the three-mode theory.

Setting $\Delta = 0$ allows one to identify this pseudo-cut-off frequency. The sign of Δ determines the nature of the roots of the cubic equation as follows:

- If $\Delta < 0$, then the equation has one real root and two non-real complex conjugate roots.
- If $\Delta = 0$, then the equation has a multiple root and all its roots are real.
- If $\Delta > 0$, then the equation has three distinct real roots.

Equation (17) is indeed a cubic equation in terms of k^2. This explains why $\Delta = 0$ corresponds to a mode transition point, and it is for this reason that the author names it the pseudo cut-off frequency.

5.3.2. Frequency responses of the uniform rod. Figure 11 shows the receptance frequency responses (displacement per unit force) of the example uniform rod. Each response plot contains four response curves, with dotted and dash dotted lines denoting responses obtained using the elementary and Love theories, and dashed and solid lines representing responses from the Mindlin–Herrmann and the three-mode theories, respectively. The frequency responses are examined over a broad frequency range of 0 to 45 kHz. The responses are presented in three separate graphs by equally dividing the frequencies.

It can be seen that the elementary and Love theories agree with each other up to a quite high-frequency range, about 20 kHz. The Mindlin–Herrmann and the three-mode theories agree with each other to an even higher frequency of about 30 kHz. However, the discrepancy between these two groups appears quite early (around the third mode, or 2 kHz).

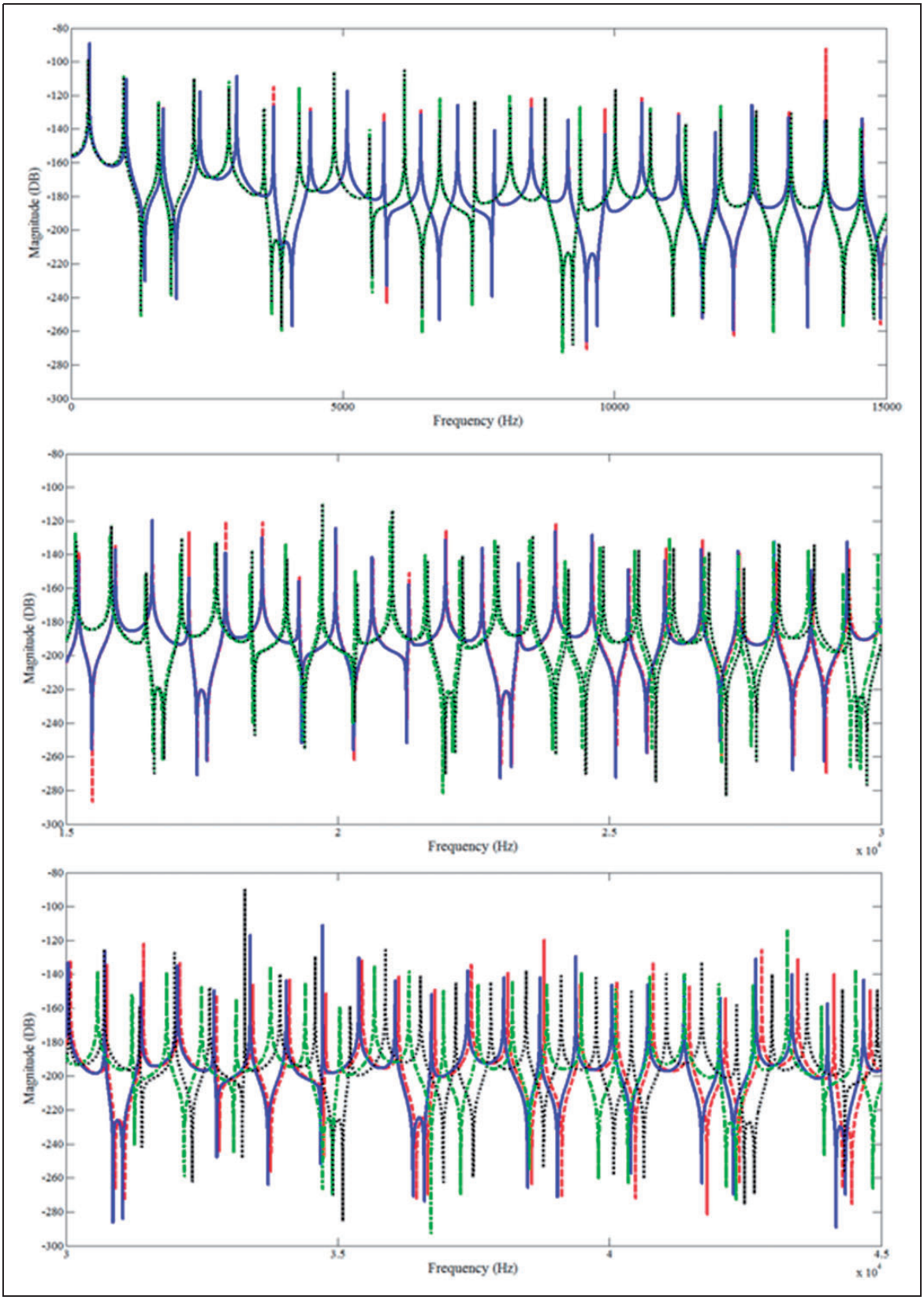

Figure 11. Receptance frequency responses of the uniform rod by the elementary (. . .), Love (-.-.-), Mindlin–Herrmann (—), and three-mode (—) theories.

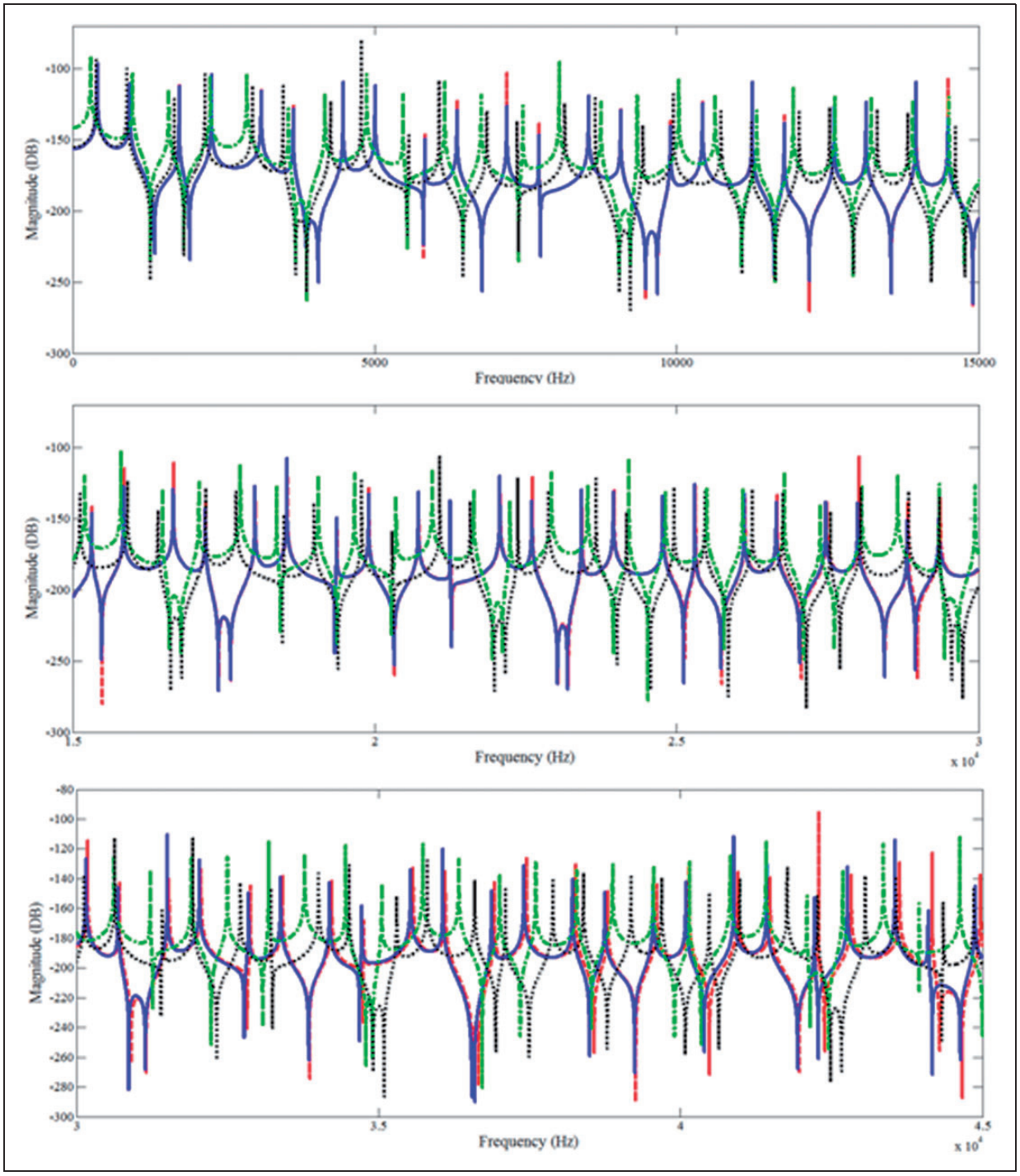

Figure 12. Receptance frequency responses of the stepped rod by the elementary (. . .), Love (-.-.-), Mindlin–Herrmann (—), and three-mode (—) theories, respectively.

5.3.3. Frequency responses of the stepped rod. Figure 12 shows the receptance frequency responses of the example stepped rod. Again each response plot contains four response curves, with dotted and dash dotted lines denoting responses obtained using the elementary and Love theories, and dashed and solid lines representing responses from the Mindlin–Herrmann and the three-mode theories, respectively.

It can be seen that the Mindlin–Herrmann and the three-mode theories agree with each other up to a high value of about 30 kHz, the same as what was observed on the uniform rod. However, the elementary and Love

theories are seen to disagree with each other even for the first mode of vibration. It is difficult to tell which one is a better approximation, as their closeness to the resonances obtained from the Mindlin–Herrmann and the three-mode theories varies.

6. Conclusions

Vibrations in uniform and stepped rods are analyzed using the four available rod theories from a wave standpoint. The wave propagation, reflection, and transmission relations are derived. Assembling these relations provides a concise and systematic approach to vibration analysis of rods. The forced response analysis results of both the uniform and stepped rods suggest that the Mindlin–Herrmann theory be used for low- to mid-frequency analysis. Within this frequency range, the mathematical complication of the three-mode theory does not offer much benefit. However, for high-frequency applications, such as that of non-destructive structural health monitoring, the three-mode theory is recommended. The discrepancies between the Mindlin–Herrmann theory and the three-mode theory become significant at high frequencies.

Another interesting finding of this paper is the so-called pseudo cut-off frequency of the three-mode theory. Similar to the two well-known cut-off frequencies, wave mode transition also occurs at this pseudo-cut-off frequency. This pseudo-cut-off frequency is related to the characteristic equation and can be solved from the discriminant of the cubic characteristic equation in k^2.

Acknowledgement

The author would like to thank the University of Michigan for providing the Flux high-performance computing system.

Funding

This work was supported by the Civil, Mechanical and Manufacturing Innovation Division of the National Science Foundation (grant number 0825761).

Nomenclature

A	cross-sectional area
$a_i^{\pm}$, $b_i^{\pm}$, $c_i^{\pm}$, $d_i^{\pm}$	positive and negative going wave components, $i = 1, 2, 3$
$\mathbf{a}^{\pm}$, $\mathbf{b}^{\pm}$, $\mathbf{c}^{\pm}$, $\mathbf{d}^{\pm}$	wave vectors
b	rod width
E	Young's modulus
$\bar{F}$	externally applied point force
$f(x)$, $\mathbf{f}(x)$	propagation coefficient/matrix for a distance x
h	rod thickness
I	geometric moment of the rod cross section
J	polar moment of inertia of the rod cross section
k	wavenumber
K_1, K_2	material parameters in Mindlin–Herrmann theory, they are related by $K_2 = K_1\left(\frac{1+\nu}{0.87+1.12\nu}\right)^2$ (Doyle, 1989), K_1 is set to unity to match the cut-off frequency between the Mindlin–Herrmann theory and the three-mode theory
L	distance
N, P	coefficients relating amplitudes of various wave components
q, $\mathbf{q}$	coefficient/vector related to point force excited waves
r, $\mathbf{r}$	reflection coefficient/matrix
t, $\mathbf{t}$	transmission coefficient/matrix (please note that t also refers to time, where it appears in one of the following forms, (x, t), $e^{i\omega t}$, or $\frac{\partial^n}{\partial t^n}$.)
$u(x, t)$	longitudinal deflection of the centerline of the rod
x	position along the rod axis

Greek symbols

μ	Lame constant, $\mu = \frac{E}{2(1+\nu)}$
λ	Lame constant, $\lambda = \frac{\nu E}{(1+\nu)(1-2\nu)}$
ν	Poisson's ratio
ρ	mass density
$\psi(x, t)$	transverse contraction of the rod
$\phi(x, t)$	parabolic distribution function of the axial displacement along the thickness of the rod
ω	circular frequency
ω_c	cut-off circular frequency

Subscripts

L, R	left and right side of a discontinuity

Superscripts

$+$, $-$	positive and negative going waves
L, R	left and right side of a discontinuity

References

Cremer L, Heckl M and Petersson BAT (2005) *Structure-borne Sound: Structural Vibrations and Sound Radiation at Audio Frequencies*, 3rd edn. Berlin: Springer-Verlag.

Doyle JF (1989) *Wave Propagation in Structures*. New York: Springer-Verlag.

Graff KF (1975) *Wave Motion in Elastic Solids*. Columbus, OH: Ohio State University Press.

Inman DJ (1994) *Engineering Vibrations*. New Jersey: Prentice-Hall, Inc.

Krawczuk M, Grabowska J and Palacz M (2006) Longitudinal wave propagation part I —comparison of rod theories. *Journal of Sound and Vibration* 295: 461–478.

Love AE (1927) *A Treatise on the Mathematical Theory of Elasticity*, 4th edition. New York: Dover Publications.

Mace BR (1984) Wave reflection and transmission in beams. *Journal of Sound and Vibration* 97: 237–246.

Mei C (2005) Global and local wave vibration characteristics of materially coupled composite beam structures. *Journal of Vibration and Control* 11(11): 1413–1433.

Mei C (2010) In-plane vibrations of classical planar frame structures – an exact wave-based analytical solution. *Journal of Vibration and Control* 16(9): 1265–1285.

Mei C (2013) Effects of rotary inertia, shear deformation, and joint model on vibration characteristics of single-story multi-bay planar frame structures. *Journal of Vibration and Control* . Epub ahead of print 29 March 2013.

Mei C (2012) Studying the effects of lumped end mass on vibrations of a Timoshenko beam using a wave-based approach. *Journal of Vibration and Control* 18(5): 733–742.

Meirovitch L (2001) *Fundamentals of Vibrations*. New York: McGraw-Hill Higher Education.

Mindlin RD and Herrmann G (1951) A one dimensional theory of compressional waves in an elastic rod. In *Proceedings of the First U.S. National Congress on Applied Mechanics*, Chicago, IL, pp. 187–191.

Viktorow IA (1967) *Rayleigh and Lamb Waves in Physical Theory and Applications*. New York: Plenum Press.